Calculating Rotordynamic Coefficients of Liquid Annular Seals by CFD for Vibration Analysis and Validation at the Test Rig

Christian Wagner(✉), Stephan Sinzig, Thomas Thümmel, and Daniel Rixen

Chair of Applied Mechanics, Technical University of Munich,
85748 Garching, Germany
c.wagner@tum.de
http://www.amm.mw.tum.de

Abstract. This article presents a simulation methodology for calculating rotordynamic coefficients of liquid annular seals using the open source software OpenFOAM. Therefore, stationary fluid solutions for several boundary conditions are generated to represent the rotational shaft speed, the eccentricity and the whirling motion. Analyzing the acting forces in a whirling coordinate frame leads to a simple curve fit to determine the rotordynamic seal coefficients. The CFD approach is validated with an analytical solution and the coefficients of characteristic states are compared to literature results. Finally, the methodology is applied to our test rig's geometry to calculate its dynamic behavior. The comparison between the simulated and measured behavior shows good agreement.

Keywords: Rotordynamic · Seal coefficient · Dynamic analysis

1 Introduction

Seals in compressors or pumps mostly separate different fluids or gases and pressure levels. In high rotational speed turbomachinery, contactless seals in various layouts like labyrinth, brush, floating ring, or simply gap seals are used. However, the presence of a leakage flow through the clearance in the contactless seal causes forces on the rotor system. They are generated by an unsymmetrical fluid velocity distribution in the seal gap for the vibrating or eccentered rotor.

Usually, the vibrational behavior of the rotating machinery is strongly affected by the seals. In unfavorable design configurations, they can excite the rotor to large vibrations and lead to an instability, like the 'oil-whip' phenomenon in journal bearings, see [1].

The forces in the seals are described using linearized rotordynamic seal coefficients like stiffness, damping, and inertia for specific operating points as pressure drop, preswirl, and rotational speeds. A lot of work has been done over recent

K. L. Cavalca and H. I. Weber (Eds.): IFToMM 2018, MMS 60, pp. 397–410, 2019.
https://doi.org/10.1007/978-3-319-99262-4_29

years in order to determine these coefficients by means of simulation or experiments.

This article presents a simulation methodology for calculating rotordynamic coefficients of liquid annular seals using the open source software OpenFOAM. Then, the calculated coefficients are used to simulate our seals test rig dynamic behavior by means of a secondary structural simulation. The comparison to measured data confirms the approach of the methodology.

Since rotational speeds and pressures are increased in technical applications, investigations in industry and academia are applied to model and identify the dynamics of rotor seal systems. Among the first in modeling the rotordynamic seal behavior using linearized coefficients were Black [2] and Childs [3], who developed and solved the bulk-flow equations to create analytical solutions for short seals. Muszynska [1,4] improves these seal models by adding eccentricity effects.

Dietzen [5] and Nordmann [6] solved the fluid equations by means of finite difference techniques. Using a rotating coordinate system leads to a stationary formulation of the whirling seal rotor.

Others, such as Kwanka [7,8] and Deckner [9,10], use CFD calculations to determine the rotordynamic seal coefficients. They also include experimental investigations using Active Magnetic Bearings (AMB) in flexible rotor-seal systems/test rigs similar to [11–14], or [15]. Examples of the use of levitating rotor test rigs to analyze seals are given by [16,17].

The fundamentals of rotordynamics, modeling, and simulation are well described in [18–20].

2 Dynamics of Rotor Seal Systems

For the sake of clarity, we write the formulation and the analysis of the rotor seal system here again, which is already presented in [21]. In the following, the Jeffcott/Laval rotor model is used to described the dynamic behavior of the system. Like the investigations of Black [2], Childs [20], and Muszynska [19], the seals are modeled using rotordynamic seal coefficients.

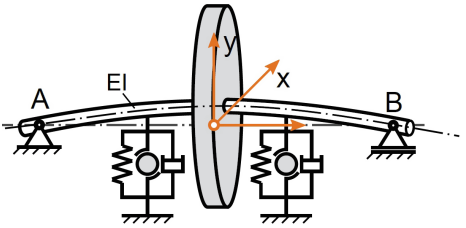

Fig. 1. Rotor seal model

2.1 Rotor Seal Model

The simplified rotor seal model, see Fig. 1, consists of a linear elastic, massless shaft with a mass disk supported by two rigid bearings. The seals, represented by their rotordynamic coefficients (mass, stiffness, and damping) are directly connected to the shaft. Using the rotor displacement $[x\ y]^T$ and projecting all forces on the disk, the equation of motion is as follows:

$$\begin{bmatrix} m_r + m_{xx} & 0 \\ 0 & m_r + m_{yy} \end{bmatrix} \begin{bmatrix} \ddot{x} \\ \ddot{y} \end{bmatrix} + \begin{bmatrix} c_{xx} & c_{xy} \\ c_{yx} & c_{yy} \end{bmatrix} \begin{bmatrix} \dot{x} \\ \dot{y} \end{bmatrix} + \begin{bmatrix} k_r + k_{xx} & k_{xy} \\ k_{yx} & k_r + k_{yy} \end{bmatrix} \begin{bmatrix} x \\ y \end{bmatrix} = \mathbf{h} \tag{1}$$

where m_{xx}, c_{xx}, and k_{xx} are the seal coefficients of direct mass, damping, and stiffness of the seals. c_{xy} and k_{xy} are the cross coupled damping and stiffness, same for the y direction, respectively. $m_r = 9.5$ kg is the rotor's mass and $k_r = 0.436$ MN/m is the shaft stiffness. The equivalent forces $\mathbf{h} = \mathbf{h}_u + \mathbf{h}_e$, representing the unbalance force, external forces, and so forth, are used to couple different models (bearings etc.) and excitations. Therefore the rotor's first (sealless) natural frequency is denoted by $\omega_1 = \sqrt{\frac{k_r}{m_r}}$.

The seal coefficients can be determined using measurements, numeric simulations, or simplified analytical solutions. In this research, the coefficients are numerically calculated using CFD simulations carried out by OpenFOAM.

2.2 Dynamic Behavior

The dynamic behavior of the rotor seal system is analyzed by its eigenvalues. Therefore, for the coupled symmetric ($*_{xx} = *_{yy}, *_{xy} = -*_{yx}$) system (rotor + seals), according to [18,21], we write:

$$\begin{bmatrix} M & 0 \\ 0 & M \end{bmatrix} \begin{bmatrix} \ddot{x} \\ \ddot{y} \end{bmatrix} + \begin{bmatrix} C & c \\ -c & C \end{bmatrix} \begin{bmatrix} \dot{x} \\ \dot{y} \end{bmatrix} + \begin{bmatrix} K & k \\ -k & K \end{bmatrix} \begin{bmatrix} x \\ y \end{bmatrix} = \mathbf{h} \tag{2}$$

For improved readability, the summarized coefficients are:

$$M = m_r + m_{xx}$$

$$C = c_{xx} = c_{yy}; \qquad c = c_{xy} = -c_{yx}$$

$$K = k_r + k_{xx}; \qquad k = k_{xy} = -k_{yx}$$

The cross-coupled terms k and c lead to tangential forces, which are destabilizing the system by transmitting energy from the rotor's rotation to the bending motion. Assuming a symmetrical rotor system, we substitute x and y with complex coordinates $z = x + jy$ and $F_z = h_x + jh_y$, where $j^2 = -1$. To determine the system's stability and its natural frequencies, the eigenvalues are calculated by $F_z = 0$ and $z = \hat{z}e^{\lambda t}$:

$$M\lambda^2 + C\lambda + K - j(c\lambda + k) = 0 \tag{3}$$

with $\lambda = -\delta + j\omega$. When the decay constant δ becomes negative, driven by the tangential forces above the system's stability limit, instability occurs. Note in particular that the coefficients are nonlinear functions of the rotational speed, the fluid properties, and the eccentricity (almost linear for $\epsilon < 0.5$).

3 Seal Simulation

In this research, the seals are analyzed by CFD. The objective is to calculate the forces acting on the rotor and to deduct rotordynamic coefficients of the seal. Knowledge of the rotordynamic coefficients allows us to investigate the behavior of the entire rotor system in an additional simulation. In order to calculate the rotordynamic coefficients, the time-dependent problem of a vibrating rotor inside a seal gap is transformed into a stationary formulation. The fluid flow and pressure distribution are calculated from the geometry and boundary conditions. Integrating the pressure distribution on the surface leads to the seal forces and, therefore, to the rotordynamic coefficients.

3.1 CFD Approach

The fluid flow inside the seal gap is a pressure and shear-driven problem. The fluid flow's motion is described exactly by the Navier-Stokes equations. For the assumed incompressible fluid (temperature and density are constant and Mach-number is less than 0.3) the momentum equation reads, according to [22]:

$$\rho \left(\frac{\partial \mathbf{v}}{\partial t} + (\mathbf{v} \cdot \nabla)\mathbf{v} \right) = -\nabla p + \mu \Delta \mathbf{v} + \mathbf{f} \tag{4}$$

The conservation of mass leads to the continuity equation:

$$\nabla \mathbf{v} = 0 \tag{5}$$

If the expected Reynolds number exceeds 2,300 within the simulation, turbulent flows need to be considered. There are multiple opportunities to solve the equations for turbulent flows. In this research, we applied the Reynolds-Averaged Navier-Stokes equations (RANS). The RANS equations are obtained by replacing every term of the Navier-Stokes equation with a constant and a fluctional expression. Finally, the equations are averaged by time. The governing equation can be treated as laminar flow, with exception of the Reynolds stress tensor:

$$-\frac{\partial \overline{u_i^* u_j^*}}{\partial x_j}$$

The Reynolds stress tensor must be modeled using averaged quantities only. In this research, we used the model of eddy viscosity, which states that the influence of turbulence is analogue to molecular viscosity. The basic $k-\epsilon$-model is applied to specify the eddy viscosity as a functional expression of the turbulent energy and the turbulent dissipation.

In case of the eccentric shaft, no geometric symmetries can be found. Hence, the simulation is bound to be three dimensional. The smooth seal is described by its diameter, clearance, and length. A structured mesh of hexahedral elements was designed, because of the seal's simple geometry, see Fig. 2. For sure, more complex geometries can be investigated as well. The spatial discretization scheme is the finite-volume-method.

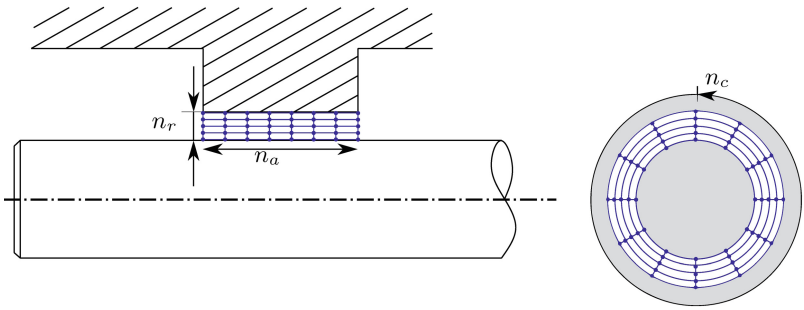

Fig. 2. Discretization of the seal: number of cells in axial direction n_a, in radial direction n_r and in circumferential direction n_c

3.2 Coordinate Transformation: Calculate Rotordynamic Coefficients

The rotordynamic coefficients link the acting forces on a rotor to the shaft's displacement, velocity, and acceleration, respectively. The quantities that describe the shaft's movement are defined within the initial coordinate frame I at the bearing center line $A - B$, as stated before. In the seal CFD analysis, a moving coordinate system with origin C in the geometric center of the rotor is used to describe the forces and movement. The movement is assumed to be a circle with radius $\epsilon = |\mathbf{r}_C|$ around center O. The coordinate system rotates with the angular whirl frequency $\omega = \dot{\psi}_C = const.$, see Fig. 3. This leads to expressions for displacements, velocities, and accelerations, respectively:

$$\begin{pmatrix} x \\ y \end{pmatrix} = \begin{pmatrix} \epsilon \cos(\omega t) \\ \epsilon \sin(\omega t) \end{pmatrix}$$

This results in different quantities of the wall velocities v (rotor and stator surface in the rotating coordinate frame) with the shaft speed $\Omega = \dot{\psi}_R = const.$:

$$v_{rotor} = (\Omega - \omega)\ \frac{D}{2}$$

$$v_{stator} = -\omega\ (\frac{D}{2} + c_r)$$

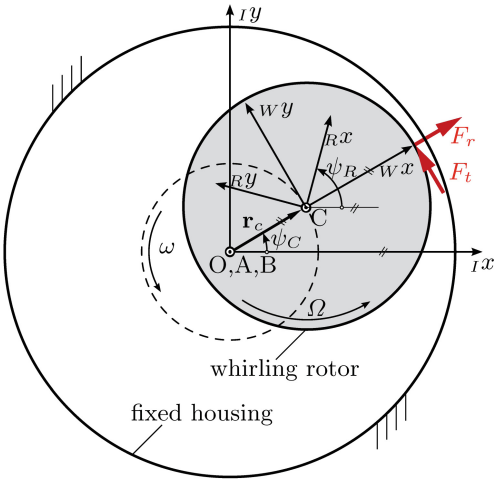

Fig. 3. Coordinate transformation and forces

with the rotor diameter D and the radial seal clearance c_r. The forces are represented in the rotating coordinate frame as well:

$$\begin{pmatrix} F_x \\ F_y \end{pmatrix} = \begin{pmatrix} F_r \cos(\omega t) - F_t \sin(\omega t) \\ F_r \sin(\omega t) + F_t \cos(\omega t) \end{pmatrix}$$

with the acting tangential and radial force, F_t and F_r. Thus, equation (1), which defines the rotordynamic coefficients, is no longer time dependent, but dependent on the whirl frequency ω and the eccentricity $\epsilon = |\mathbf{r}_C|$:

$$\begin{pmatrix} -\frac{F_r}{\epsilon} \\ -\frac{F_t}{\epsilon} \end{pmatrix} = \begin{pmatrix} -m_{xx}\omega^2 + c_{xy}\omega + k_{xx} \\ c_{xx}\omega - k_{xy} \end{pmatrix} \tag{6}$$

The spatial movement of the shaft within the CFD simulation is described with boundary conditions only.

Now, it is possible to calculate the rotordynamic coefficients if there are simulated forces on hand for several whirl frequencies. There have to be at least three different simulations at different whirl frequencies, since the radial part of the force is a polynomial of second order with respect to the whirl frequency. The velocity at inlet and outlet surfaces has a zero gradient. Besides the boundary condition describing the velocity, there are boundary conditions for the pressure: At the inlet, the presetting of the total pressure ($p_0 = p + \frac{1}{2}\rho u^2$) is given. At the outlet, the dynamic pressure is set to zero. In this work, we employed the algorithm SIMPLE (Semi-Implicit Method for Pressure Linked Equations) to solve the RANS-equations. This algorithm iteratively calculates the pressure distribution and the velocity distribution alternately. The solution from one field serves as the initial value for the other. Finally, Eq. (6) was fitted to the simulated values of the forces to calculate the rotordynamic coefficients.

4 Experimental Setup

This section describes the experimental setup for analyzing rotor seal systems at the Chair of Applied Mechanics at the Technical University of Munich, as in [21]. First, the seals test rig is presented, then the dynamic behavior is analyzed and compared to the simulation results.

The experimental analysis is examined on the seals test rig (see Fig. 4). The main components are a flexible shaft and a mass disk (1) with two symmetrically-arranged liquid annular seals (2) in the middle (see details in Fig. 5). Eddy current sensors for measuring the displacement (6) and a piezo force platform (7) are arranged in the seals stator housing (8). The fluid is injected between the two seals with a maximum pressure of 100 bar. The rotor runs at over-critical speed above the first (sealless) natural frequency ω_1 up to 12,000 rpm. An active magnetic bearing (3) is used as an exciter (2D shaker) at the shaft. The rotor shaft is supported by two ball bearings (4) and driven by a servo motor (5). The typical test procedure is the stationary rotor run-up (discrete rotational speeds) with or without AMB excitation. Therefore, the test rig is controlled and the signals are measured using a dSpace 1103 system (10 kHz sampling rate), see [12,21].

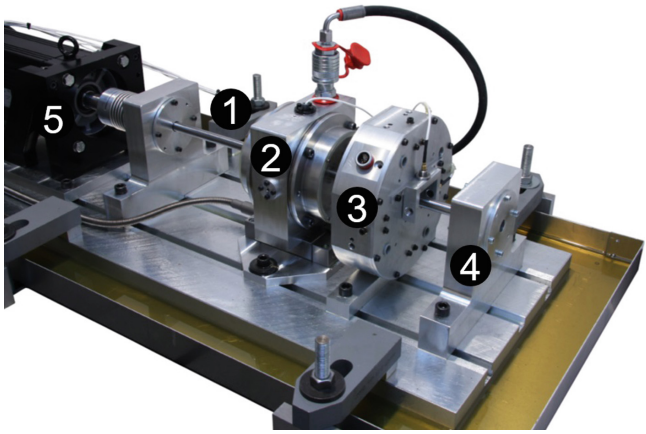

Fig. 4. Seals test rig

5 Validation and Dynamic Analysis

In this section, the CFD simulation methodology is validated. Therefore, an analytical solution is derived from the Navier-Stokes equations to define the numerical errors with respect to simple geometries. Additionally, the calculated rotordynamic coefficients are compared with those published by Dietzen and

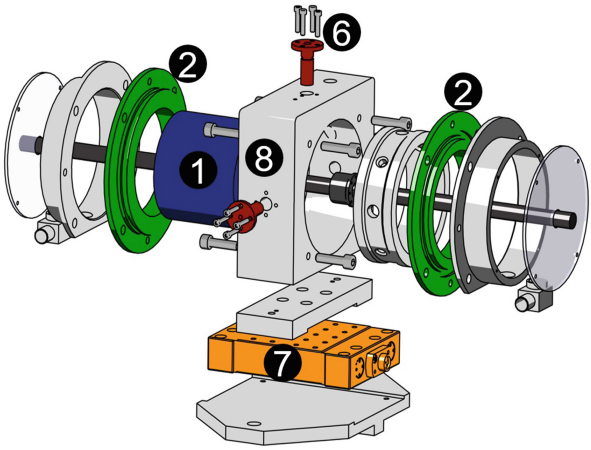

Fig. 5. Seals housing detail

Nordmann [5]. Afterwards, the geometry of the presented seals test rig configuration is simulated so that its vibrational behavior can be compared to experimental results.

5.1 Validation by an Analytical Solution

The numerical convergence of both the discretization scheme and the solving process has to be proved by applying the boundary conditions and the fluid properties for different grid resolutions. Thus, an analytical expression of the pressure and velocity distribution is generated. The analytical solution is only available if the Navier-Stokes equations are simplified by some assumptions. Hence, the configuration is stated to be time independent, to be a plain annular seal, to assume a centric rotor, to have no circumferential velocity, and to be laminar flow. These assumptions lead to a linear equation of the pressure distribution in axial direction:

$$p(z) = \frac{p_o - p_i}{l} z + p_i$$

with the pressure at inlet and outlet, p_i and p_o. A quadratic equation of the velocity distribution in radial direction follows as:

$$u_z(r) = \frac{p_o - p_i}{4\mu l} \left(\left(r^2 - r_i^2\right) + \left(r_o^2 - r_i^2\right) \frac{ln\left(\frac{r_i}{r}\right)}{ln\left(\frac{r_o}{r_i}\right)} \right)$$

where r_i and r_o denote the inner (i.e. the rotor) and outer radial wall coordinate. The axial velocity u_z is integrated over the cross section of the gap to gain an expression of the volume flow through the seal. A second-order Taylor-series approximation of the integrated expression yields a term for the leakage $\dot{V}$, also found in [18]:

$$\dot{V} = \frac{\Delta p d_m \pi h_0^3}{12 \nu l} \tag{7}$$

The difference between a simulated value of the volume flow and Eq. (7) represents a quantity of the numerical error. The criteria for proving convergence of a scheme is that the numerical error decreases for an increasing number of cells. This was demonstrated (length: 20 mm, diameter: 1,000 mm, clearance: 0.17 mm):

- **3D case 1:** 4,000 cells (in axial direction $n_a = 10$, in radial direction $n_r = 4$, and in circumferential direction $n_c = 100$), deviation of 20%
- **3D case 2:** 63,000 cells ($n_a = 25$, $n_r = 10$, $n_c = 252$), deviation of 8%

In this special case, the rotor is assumed to be placed centrically as mentioned before. This symmetry can be exploited to handle the configuration as a two-dimensional one. Thus, a sector of the circumference is simulated only. Namely, $\frac{1}{1{,}000}$ of the geometry is discretized using one cell in circumferential direction, so $n_c = 1$. The volume flow calculated is subsequently multiplied by 1,000. Again, two different cases are analyzed to prove the convergence:

- **2D case 1:** 2,000 cells ($n_r = 20$, $n_a = 100$), deviation of 0.5%
- **2D case 2:** 8,000 cells ($n_r = 40$, $n_a = 200$), deviation of 0.03%

5.2 Validation by Published Rotordynamic Coefficients

An example of validating the CFD approach with published rotordynamic seal coefficients is given in [5]. Water flows through a plain annular seal. The resulting flow is going to be turbulent, since the pressure boundary conditions lead to a Reynolds number of more than 2,300. Hence, the RANS equations are solved numerically. The eddy viscosity is modelled using the $k-\epsilon$ model. The simulation is characterized by the following parameters:

- **Dimensions:** length: 23.5 mm, diameter: 57 mm, and clearance: 0.2 mm
- **Fluid:** density: 996 kg/m^3, dynamic viscosity: $7 \cdot 10^{-4}$ kg/ms
- **Boundary conditions:** total pressure drop: 4.5 bar, inlet loss ratio: 0.5, preswirl ratio: 0.5
- **Simulation case:** 27,264 cells ($n_a = 12$, $n_r = 8$, and $n_c = 284$), expected numerical deviation is 8–20%

Unfortunately, in [5] there is no boundary condition for the turbulence intensity given at the inlet. The assumption for the turbulence intensity within this study is 5%. It was brought to light that the scale of turbulence intensity at the inlet influences the results to a not-insignificant degree. The results show a mean difference of about 20% between the simulation and the published values, see Fig. 6.

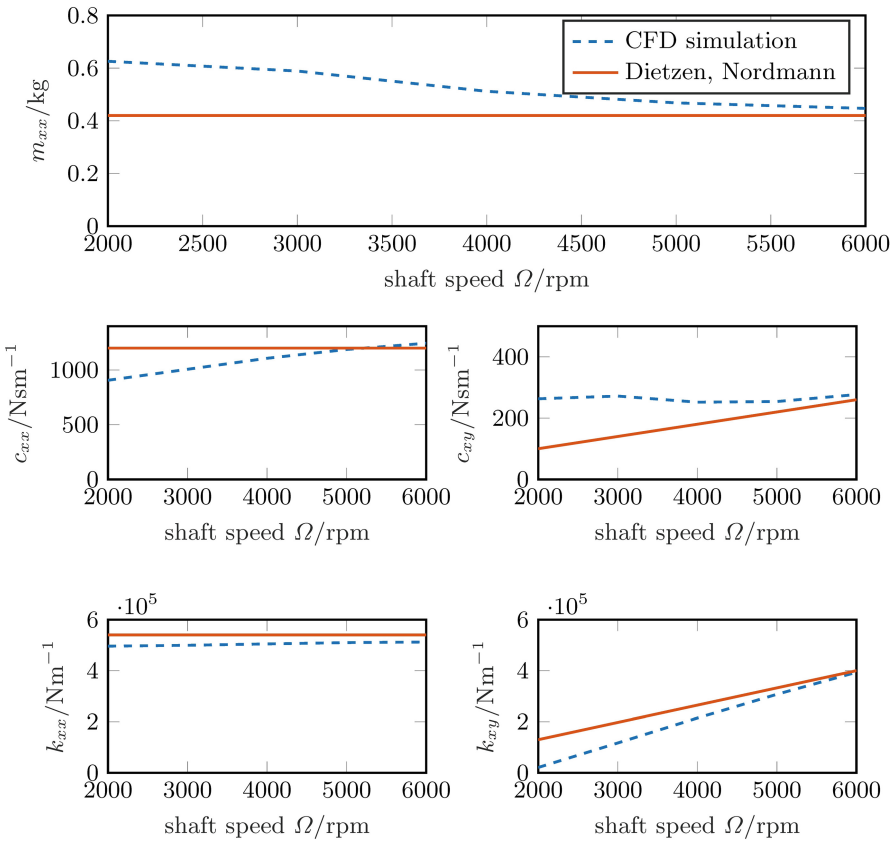

Fig. 6. Coefficients calculated by [5], comparison with CFD analysis approach

Table 1. Test rig and fluid parameters

	Name	Value
Rotor	Shaft	15 × 600 mm
	Mass	9.5 kg
	1^{st} seal-less natural freq.	34.1 Hz
Seal	Diameter	100 mm
	Length	20 mm
	Clearance	0.17 mm
	Pressure	200 kPa
	Dyn. viscosity	40.48 $\cdot 10^{-3}$ N·s/m^2
	Density	880 kg/m^3

5.3 Dynamic Analysis of the Test Rig

At the presented test rig, a run-up is performed with the parameters in Table 1.

The waterfall plot in Fig. 7 shows the two side spectra of the rotor's displacement signal at several rotational speeds. The 'dry' (without seal) 1st natural frequency is at 34.1 Hz and cannot be seen anymore. At this time, for safety reasons, the measurements were only up to 7,000 rpm, due to the large vibration amplitudes of the rotor at its natural frequency ω_{1f} (the forward whirl'), which is significantly higher than the unbalance response Ω.

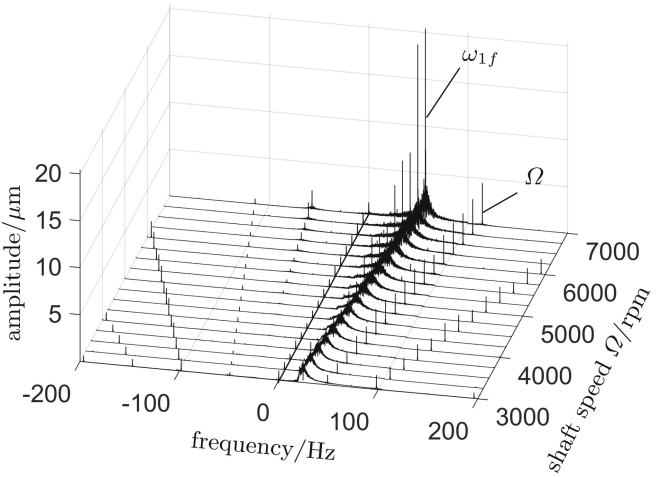

Fig. 7. Full spectrum waterfall plot of the measured test rig run-up

The whirl-frequency ratio is almost $\omega_{1f}/\Omega \approx 0.4888$ for higher rotational speeds. The backward whirl natural frequency ω_{1b} cannot be seen here because of its low excitation and the high damping.

The CFD analysis procedure described is applied to the seals geometry of the test rig to calculate its rotational speed-dependent rotordynamic coefficients. Therefore, one seal is discretized with 4,000 cells ($n_a = 10$, $n_r = 4$, and $n_c = 100$), the expected numerical deviation is 20%. The seal coefficients are then coupled to the 'dry' rotor parameters to analyze the system's rotational speed-dependent eigenvalues. The Campbell diagram in Fig. 8 shows the simulated 1st natural frequency in forward whirl direction ω_{1f} compared to the frequency measured. The whirl frequency ratio of the simulated system is $\omega_1/\Omega \approx 0.4909$, which yields a difference of 0.42%.

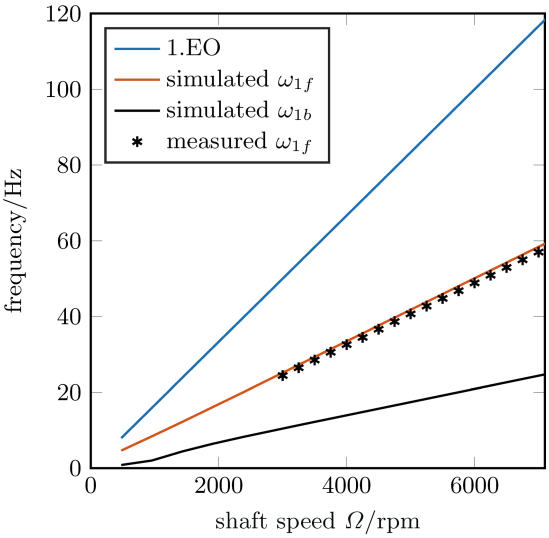

Fig. 8. Campbell diagram of the simulated and measured test rig

5.4 Comparison and Analysis of the Results

The outlined CFD approach was confirmed by the validation. The analytical solution can be used for simple cases to determine the expected numerical simulation errors of the grid used. Thus, the rotordynamic seal coefficients calculated are within the numerical deviation compared to literature values. The calculation of the test rig's natural frequencies using the simulated coefficients shows a very good agreement with those of the experiment.

6 Conclusion: Summary and Outlook

In this research, a methodology for determining the rotordynamic coefficients of seals by CFD simulation is presented. To show the numerical errors of the discretization and the solving process, an analytical and, thus, exact solution is used for a simple case. The error rate of the 3D discretization is approximately 8% of the exact solution, the refined 2D case has a deviation of 0.003%. This confirms the discretization, the setup of the boundary conditions, and the solving process. The rotordynamic seal coefficients are calculated using stationary CFD simulations in a whirling coordinate frame. For various values of the rotational speed, different whirl frequencies are applied to simulate the forces acting on the rotor. A least squares fit of the tangential and the radial forces, depending on the whirl frequency, leads to the coefficients. The coordinate transformation, post processing, and finally the calculated rotordynamic coefficients, are validated by a literature example (Dietzen and Nordmann). Finally, the presented methodology is used to simulate the dynamic behavior of our seals test rig. The natural

frequency calculated (whirl frequency ratio) shows a good agreement with the measured test rig data. Future work will be made up of detailed experimental determination of coefficients and investigations in eccentricity/tilting effects.

Acknowledgments. This project is supported by the Ludwig Bölkow Campus and the Bavarian State. The friendly and effective cooperation between the partners of the research project is much appreciated.

References

1. Muszynska, A.: Whirl and whiprotor/bearing stability problems. J. Sound Vibr. **110**(3), 443–462 (1986)
2. Black, H.F., Jenssen, D.N.: Black, Jenssen 1969-70 - Dynamic Hybrid Bearing Characteristics. In: Proceedings of the Institution of Mechanical Engineers, Conference Proceedings, vol. 184-14, pp. 92–100. SAGE Publications, Sage UK, London (1969)
3. Childs, D.W.: Dynamic analysis of turbulent annular seals based on hirs' lubrication equation. ASME Lubr. Technol. **105**, 429–436 (1983)
4. Muszynska, A.: Improvements in lightly loaded rotor/bearing and rotor/seal models. J. Vibr. Acoust. Stress Reliab. Des. **110**, 129–136 (1988)
5. Dietzen, F.J., Nordmann, R.: Calculating rotordynamic coefficients of seals by finite- difference techniques. Trans. ASME J. Tribol. **109**, 388–394 (1987)
6. Nordmann, R., Dietzen. F.J.: Finite difference analysis of rotordynamic seal coefficients for an eccentric shaft position. In: NASA, Lewis Research Center, Rotordynamic Instability Problems in High-Performance Turbomachinery, Kaiserslautern University, Department of Mechanical Engineering, no. N89-22906, pp. 269–284 (1989)
7. Kwanka, K.: Dynamic coefficients of stepped labyrinth gas seals. J. Eng. Gas Turbines Power **122**, 473–477 (1999)
8. Kwanka, K., Sobotzik, J., Nordmann, R.: Dynamic coefficients of labyrinth gas seals: a comparison of experimental results and numerical calculations. In: Proceedings of ASME Turbo Expo (2000)
9. Deckner, M.: Eigenschaften kombinierter Labyrinth - Bürstendichtungen für Turbomaschinen. Doktorarbeit, Technischen Universität München (2009)
10. Gaszner, M.: Rotordynamische Charakterisierung von Dichtungssystemen zur Anwendung in Kraftwerksdampfturbinen. Ph.D. thesis, Technical University of Munich (2015)
11. David, J.G.M., Thiago, G.R., Fernando, A.N.C.P.: Identification of rotordynamic seal coefficients by means of impedance matrix and an optimization strategy. In: Proceedings of the XVII International Symposium on Dynamic Problems of Mechanics, São Sebastião, SP, Brazil. ABCM (2017)
12. Wagner, C., Tsunoda, W., Matsushita, O., Berninger, T., Thümmel, T., Rixen, D.: Prediction of instability in rotor-seal systems using forward whirl magnetic bearing excitation. J. Tech. Mech. **37**(2–5), 358–366 (2017)
13. Wagner, C., Tsunoda, W., Berninger, T., Thmmel, T., Rixen, D.: Instability prediction and rotordynamic with seals: simulations based on the bulk-flow theory and experimental measurements. In: XVII International Symposium on Dynamic Problems of Mechanics DINAME, São Sebastião, SP, Brazil. ABCM (2017)

14. Ha, T.W., Choe, B.S.: Numerical simulation of rotordynamic coefficients for eccentric annular-type-plain-pump seal using CFD analysis. J. Mech. Sci. Technol. **26**(4), 1043–1048 (2012)
15. Kim, S.H., Ha, T.W.: Prediction of leakage and rotordynamic coefficients for the circumferential-groove-pump seal using CFD analysis. J. Mech. Sci. Technol. **30**(5), 2037–2043 (2016)
16. Zutavern, Z.S.: Identification of rotordynamic forces in a flexible rotor system using magnetic bearings identification of rotordynamic forces in a flexible rotor system using magnetic bearings. Ph.D. thesis, Texas AM (2006)
17. Santos, I.F., Svendsen, P.K.: Noninvasive parameter identification in rotordynamics via fluid film bearings—linking active lubrication and operational modal analysis. J. Eng. Gas Turbines Power **139**(6), 062507 (2017)
18. Gasch, R., Nordmann, R., Pfützner, H.: Rotordynamik. Springer, Heidelberg (2002)
19. Muszynska, A.: Rotordynamics. CRC Press, Boca Raton (2005)
20. Childs, D.W.: Turbomachinery Rotordynamics. Wiley-Interscience, Dallas (1993)
21. Wagner, C., Thümmel, T., Rixen, D.: Experimental prediciton of instability in rotor seal systems using output only data. In: International Symposium on Transport Phenomena and Dynamics of Rotating Machinery ISROMAC 2017, Maui, Hawaii (2017)
22. Spurk, J.H., Nuri, A.: Strömungslehre - Einführung in die Theorie der Strömungen (2010)